BOUNDED PLASMA DYNAMICS FROM PARTICLE SIMULATIONS; MOVIE SCRIPT

by

C. K. Birdsall, T. L. Crystal, P. C. Gray, and S. Kuhn

Memorandum No. UCB/ERL M85/54

2 July 1985

BOUNDED PLASMA DYNAMICS FROM PARTICLE SIMULATIONS; MOVIE SCRIPT

by

C. K. Birdsall, T. L. Crystal, P. C. Gray, and S. Kuhn

Memorandum No. UCB/ERL M85/54

2 July 1985

ELECTRONICS RESEARCH LABORATORY

College of Engineering
University of California, Berkeley
94720

BOUNDED PLASMA DYNAMICS FROM PARTICLE SIMULATIONS: MOVIE SCRIPT

(Plane hot emitter, cold collector, collisionless, 1-d, unmagnetized)

C. K. Birdsall, T. L. Crystal, P. C. Gray, S. Kuhn*

Plasma Theory and Simulation Group

Department of Electrical Engineering and Computer Sciences

and the Electronics Research Laboratory

University of California, Berkeley, CA 94720

Permanent address: Institute for Theoretical Physics,
University of Innsbruck, Innrain 52
A-6020 Innsbruck, Austria

Research sponsored by DOE contract DE-AS03-76-F00034-DE-AT03-76ET53064, ONR contract N00014-77-C-0578, and Varian Associates.

Abstract

The behavior in time of a plasma bounded by a plane emitter and cold collector is observed in a movie showing simultaneous plots of electron and ion phase spaces (v_x vs x), potential $\varphi(x)$, charge density $\rho(x)$ and current density $J(t)$. Using $T_i / T_e = 1$ at the emitter, $m_i / m_e = 40$, eight sequences were made for various emission ratios ($\alpha = n_{i0}^{+} / n_{e0}^{+} = 0.1$, 1.0 and 4.0). With floating bias (open circuit), the plasma has fluctuations which are small compared with average values. With ion rich emission and virtual anode, an electron hole is expected but is found to be filled. With moderate positive bias, violent instabilities are observed in great detail for both electron and ion-rich emission, associated with formation of potential minima, ejecting electrons, then repeating. The new information is the detail, allowing more complete understanding. The script provides the model, the parameters of the movie, and brief descriptions of the sequences.

Copies of the movie are available, at cost (about $80) by written request to Professor C. K. Birdsall.

Section I. Introduction

This report provides a description of the movie entitled "Bounded Plasma Dynamics from Particle Simulations," produced in the Spring of 1984 by the Plasma Theory and Simulation Group at the Electronics Research Laboratory, University of California, Berkeley, California. It was first presented at the IEEE Conference on Plasma Sciences, May 1984, (Kuhn et al., 1984a) and at the 1984 International Conference on Plasma Physics June/July 1984 (Kuhn et al., 1984b) and at the Second Symposium on Plasma Double Layers and Related Topics (Gray et al., 1984).

In order to get at plasma-wall (plasma-surface) interactions of many kinds, a bounded plasma particle simulation code was constructed in the Plasma Device Workshop, Spring 1983, called PDW1 (see Appendix A). The initial application was to single-ended plasma source devices, very much like a Q-machine, but also related to center-cell to end-plate regions in a tandem mirror machine or plasma-to-neutralizer plasma in tokamak diverters. The former are very well known from experiments and from (mostly) time-independent analysis (for example, Ott 1967, Kuhn 1981) and hence, provide a basis for comparison tests. Some very interesting fluctuations, oscillations and instabilities have been observed in single-ended source experiments (Rynn 1962, 1966, Cutler 1964, Burger 1964, 1965, 1967, Cutler and Burger 1966, Ott 1967) and are also available for comparison.

The initial simulations that we made were encouraging. The usual computer outputs of periodic sampling (snapshots of potentials, fields, densities, and phase spaces) and time histories (of energies, potentials at fixed points, etc.) were found to be mostly in agreement with existing analyses. The phase-space plots (particle velocities versus positions) were very revealing, helping to make the plasma physics clearer.

However, using a positive bias on the cold collector, the system became physically unstable so rapidly that the usual occasional snapshots were much too far apart in time. Hence we decided to make a movie (a continuous set of snapshots) simply to get at as much detail as possible of the onset and consequences of the instabilities. Once we had made one movie sequence, it became obvious that we should cover more regimes as well and hence we made the eight sequences for the whole movie. We are aware that much of the movie is rediscovery of the physics of the works referenced above; however, the movie, with its simultaneous plots of potential, charge density, electron and ion phase spaces, allows more firm explanations of onset of the positive-bias instabilities. This is the primary added contribution.

The movie shows a device eight separate runs (henceforth referred to as R1 through R8), all performed with the bounded-plasma particle code PDW1 and chosen so as to cover typical experimental situations.

The report is organized as follows. In Section II the one-dimensional, collisionless, electrostatic, single-emitter plasma diode model is briefly described. Its equilibria, the associated potential richness or (η_c, α) parameter diagram, and some of its practical implications are reviewed. In Section III the physical parameters are named. In Section IV the parameters characterizing the eight runs are listed. In Section V, short descriptions are presented for each sequence, along with sample frames from the movie. Detailed scientific evaluations are being prepared for separate publications as listed in Section VI, References. Appendix A is a short description of the code used, PDW1. Appendix B lists the computer parameters used.

Section 2. Physical Model

The model considered is a bounded electrostatic plasma, in one dimension, as shown in Figure 1. There is a single-emitter (hot plate) at x = 0 (held at

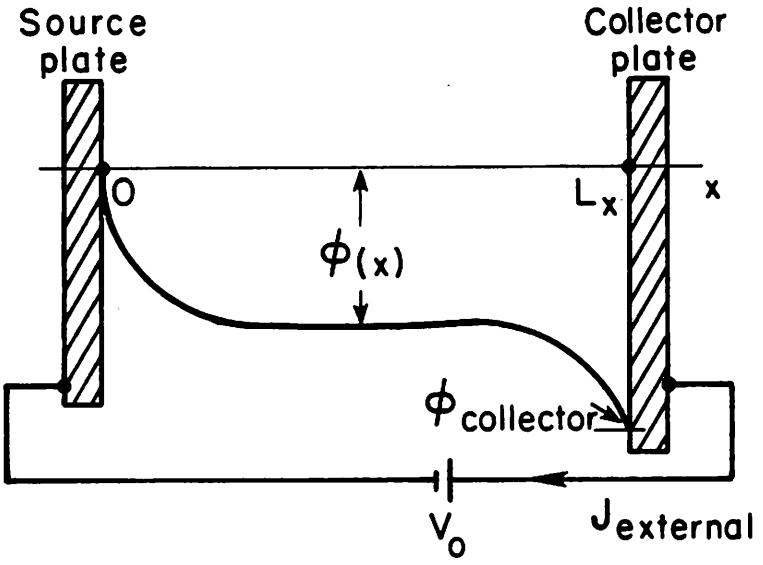

Fig 1. Planar model, showing typical potential profile. Source plate emits electrons and ions with half-Maxwellian velocities. Both plates absorb charges striking them. (The V_0 shown is negative.)

potential φ = 0, and temperature T) from which electrons and ions are emitted continuously with half-Maxwellian velocity distributions corresponding to the temperature T and with emission densities n_{e0}^{+} and n_{i0}^{+}, respectively. There is a collector (cold plate) at $x = L_x$, held at constant bias V_c or left floating (open circuit). Particles colliding with either electrode are absorbed.

The time-independent equilibria of this device have been studied by many (e.g., Ott 1967, Kuhn 1981). They may be classified in terms of the (η_c, α) parameter diagram shown in Fig. 2 where $\eta_c \equiv eV_c / kT$ and $\alpha \equiv n_{i0}^{+} / n_{e0}^{+}$. In the movie, simulation runs were made for eight parameter points (η_c, α) representative of the parameter regions 1', 2', 1, and 2.

Section 3. Physical Parameters Used

The physical parameters used are as follows. The injected particles have velocity distributions

$$f_{\sigma 0}^{+}(v) = \sqrt{\frac{2}{\pi}} \frac{n_{\sigma 0}^{+}}{v_{t\sigma}} \exp\left(-\frac{v^2}{2v_{t\sigma}^2}\right) \qquad v > 0 \tag{1}$$

where:

σ = e, i is species index

sub 0 is x = 0

super + means positive x-direction

$n_{\sigma 0}^{+}$ is injection density

$v_{t\sigma} \equiv \sqrt{\frac{kT_\sigma}{m_\sigma}}$ is thermal velocity

k = Boltzmann's constant

T = hot plate temperature ($T_i = T_e = T$)

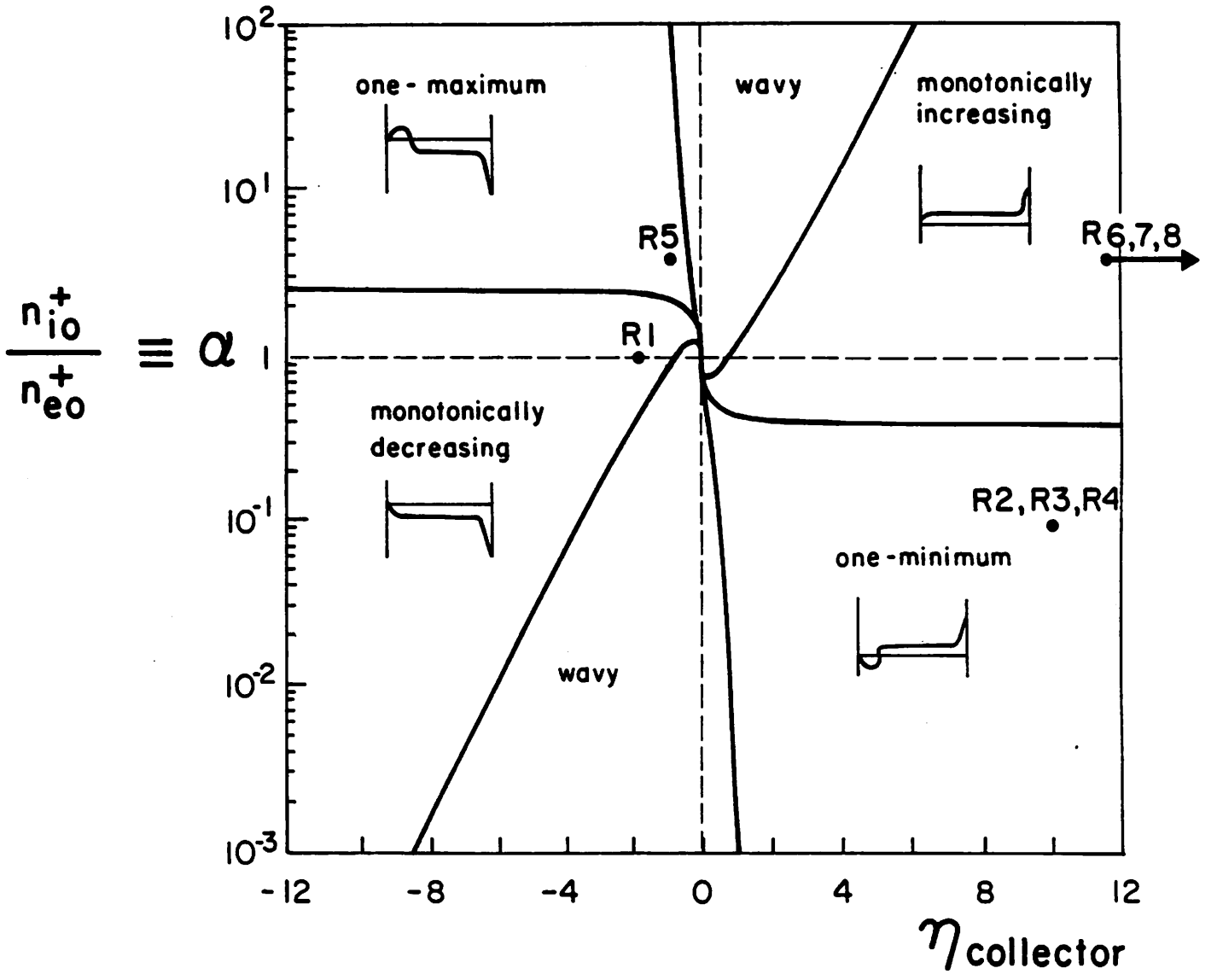

Fig 2. Parameter diagram for single-ended source and cold collector plate. The inserts are typical potential profiles for the regions. Operating points for the 8 runs are noted by R1, R2, etc.

m_σ is particle mass

$\alpha \equiv n_{i0}^{+} / n_{e0}^{+}$ emitter neutralization parameter (α>1 is ion rich;

α<1 electron rich)

The potentials used are:

$\varphi(L_x)$ = cold plate potential; (i) equal to $\varphi_{floating}$ if the device is open circuited (and fluctuating in time), (ii), equal to battery voltage V_0, if connected to the battery, fixed in time.

$\eta(x) = \frac{e\varphi(x)}{kT}$ is normalized potential

$$\eta_c \equiv \eta(x = L_x) = \eta_{collector} = \frac{e\varphi(L_x)}{kT}$$

Lastly, $\Lambda \equiv L_x / \lambda_{Deo}$ length in terms of injected electron density, temperature.

In all of the runs the mass ratio was m_i / m_e = 40 and the temperature ratio was T_i / T_e = 1.0. The lengths were either L_x = 2 or 4. The charge to mass ratio for electrons was q_e / m_e = -1.0 and for ions, q_i / m_i = 0.025.

Section IV. Summary of the Movie Parameters

The parameters for the simulation runs R1 through R8 shown in the movie were chosen so as to cover typical experimental situations. A rather global but very useful survey may be obtained by inspection of the (η_c,α) parameter diagram (Fig. 2), where the corresponding parameter points are marked R1 through R8. Table 1, along with the following description, provides a more complete and detailed compilation of the physical, numerical, and diagnostic parameters involved. Most of the symbols used here were already defined in Sec. III.

For each simulation run, the diode is empty initially (i.e., at t = 0). For $t \geq 0$, electrons and ions are constantly injected at the hot plate with particle velocities generated so as to approximate the half Maxwellian injection

distribution functions defined by Eq. (1). The diode first goes through a filling phase (initial transient), and eventually settles down at a final state, which may be more or less static or rather violently dynamic, depending on the specific experimental parameters of the run in question.

In Table 1 we have listed system, electron, ion, discretization, diagnostic, scaling, and nondimensional parameters characterizing the eight runs. (The table must not be confused with the list of input parameters to PDW1. The latter are described in detail in Appendix B).

Section V. Brief Summary of Movie Runs

Run R1. Neutral injection, α = 1, floating cold plate (open circuit, no net current).

The electrons quickly charge the collector negatively, dropping the collector potential, creating two sheaths, one at the source and one at the collector, both repelling electrons. The device is stable, but with oscillations peaked at $\omega \approx \omega_{pe}$ ($x = L_x/2$), observed at the collector (η_c = -1.84 ± 0.16, time average ± oscillations) and in the plasma region (η_p = -1.46 ± 0.13).

Computer snapshots, like the movie frame, appear as in Fig. 3. The upper parts are the electron and ion phase spaces (v_x versus x). The lower parts are the charge density and the potential, all versus x, at time t = 43.75. The average numberof electrons is about 1450 and the average number of ions is about 1250.

Run R2. Electron rich, α = 0.1, small positive bias, net current.

The electron-richness causes a potential minimum to form in front of the source (electron Debye cloud) which acts as a major control valve on the electron flow, returning most electrons to the source. When too many electrons are let in, a second potential minimum forms, disrupting the flow, expelling more than the excess electrons, with ions sloshing on a longer time scale, leading to

Table I

Physical Parameters

For all runs:

$v^+_{teo} = 1.0$

$v^+_{tio} = \sqrt{\frac{m_e}{m_i}}\ v_{te} = 0.1581$

$\frac{m_i}{m_e} = 40$, $\frac{T^+_{io}}{T^+_{eo}} = 1.0$, $\varepsilon_o = 1.0$

Run No.	R1 floating	R2/R3 E-rich ⊖ bias		R4 E-rich ⊖ bias	R5 I-rich float	R6/R7 I-rich ⊖ bias		R8 I-rich ⊖ bias
1. System Parameters								
L	2	4	4	2	2	4	4	4
kT	0.05	0.05	0.05	0.05	0.05	0.1	0.1	0.1
$V_{collector}$	floating	10	10	10	floating	60	60	150
t_{max}	50	50	50	50	50	50	50	12.5
N (steps)	6400	16,000	16,000	16,000	6400	32,000	32,000	6400
2. Electron Parameters								
m_e	0.05	0.05	0.05	0.05	0.05	0.1	0.1	0.1
q_e	-0.05	-0.05	-0.05	-0.05	-0.05	-0.1	-0.1	-0.1
n^+_{eo}	1600	3200	3200	3200	1600	1600	1600	1600
J^+_{eo}	-63.83	-127.66	-127.66	-127.66	-63.83	-127.66	-127.66	-127.66
3. Ion Parameters								
m_i	2	2	2	2	2	4	4	4
q_i	0.05	0.05	0.05	0.05	0.05	0.1	0.1	0.1
n^+_{io}	1600	320	320	320	6400	6400	6400	6400
J^+_{io}	10.09	2.018	2.018	2.018	40.37	80.74	80.74	80.74
4. Discretization Parameters								
NG(cells)	128	256	256	128	128	256	256	256
Δt	7.8125E-3	3.125E-3	3.125E-3	3.125E-3	7.8125E-3	1.5625E-3	1.5626E-3	7.8125E-4
$\omega_{peo}\Delta t$	0.07	0.04	0.04	0.04	0.07	0.02	0.02	0.02
$v_{max}\Delta t/\Delta x$	2.5	0.894	0.894	0.894	2.5	1.1	1.1	0.866
5. Diagnostic Parameters								
IPLOT(in Δt)	5	10	10	10	5	20	20	10
Lower left plot	$\rho(x)$	$\rho(x)$	J(t)	$f(v_i)$	$f(v_e)$	$\rho(x)$	J(t)	$\rho(x)$
6. Scaling Length								
λ_{Deo^+}	0.11180	7.906E-2	7.906E-2	7.906E-2	0.11180	7.906E-2	7.906E-2	7.906E-2
7. Nondimensional Parameters								
$\eta_{collector}$	floating	10	10	10	floating	60	60	150
α	1	0.1	0.1	0.1	4	4	4	4
Λ	17.89	50.6	50.6	25.3	17.89	50.6	50.6	50.6

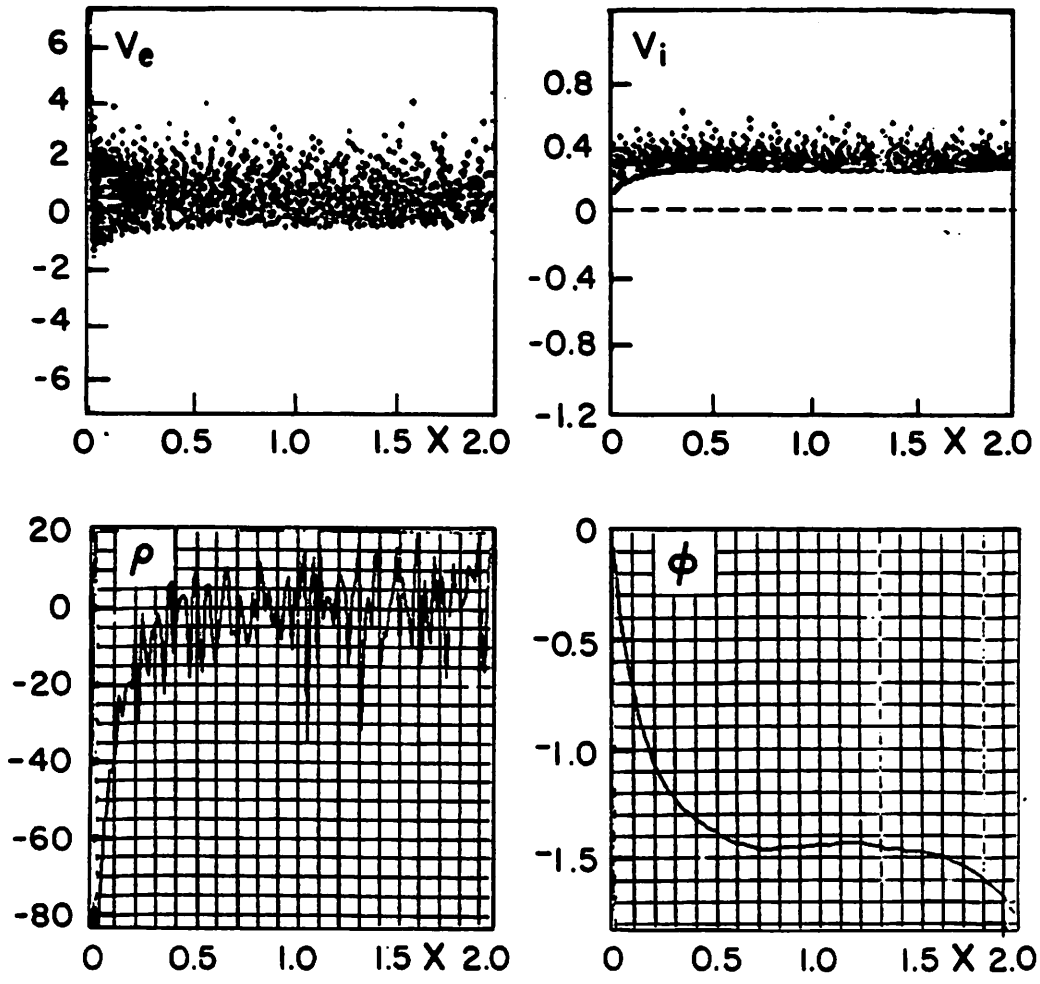

Fig 3. Run R1 at time t = 43.75 showing a typical movie frame. Electron and ion phase spaces are at the top (v_e, v_i versus x). Charge density ρ is at the lower left and potential φ at the lower right, both versus x. The collector is floating (at $\varphi \approx -1.84$), causing most electrons to be reflected back to the source. All ions are transmitted.

current having a saw-tooth relaxation like waveform, with major period $\tau \approx 14$, a little shorter than the transit time of a thermal ion $\tau \approx 25$. The rise time (just before t = 40) is close to the thermal electron transit (or filling) time. $L_x / v_{te} = 4$. (Run R3 is the same as R2, except that current density as a function of time is shown in the lower left hand corner, J(t) vs t.)

Figure 4 shows a movie frame at t = 43.75 for Run R3. The second potential minimum has formed, causing electrons to be returned, near $x \cong 1.5$, leading to an electron hole a little later in time.

The electron current injected is $J_e^+ = -127.7$, with most of that returned to the emitter by the first potential minimum. The time-average current shown here is about $J_e \cong -30$, which is about that consistent with an average value of about $\varphi \approx -1.5$ at the first minimum (i.e., -127.7 exp (-1.5) =-28.5).

While the main oscillation period is long, about a thermal ion transit time, there are some shorter periods in J(t) (see t $\cong$ 33,46) when the electrons from the second minimum reach emitter.

The Child's law current value (no ions) is calculated to be $J_{CL} = -1.24$ which is far smaller than the currents seen here (i.e., having the ions present allows for much larger currents than J_{CL}).

It is expected that longer runs would show a completely periodic ehavior, without the slow average increase seen here.

More details are given in our Budapest paper (Birdsall et al., 1985).

Run R4. Electron rich, $\alpha = 0.1$, large positive bias, net current.

There is still a potential minimum near the source, but the bias is so high as to draw out most electrons and repel most ions. There is no central plasma region. The potential minimum accelerates ions near the source, which are then repelled by the positive bias, forming an ion hole.

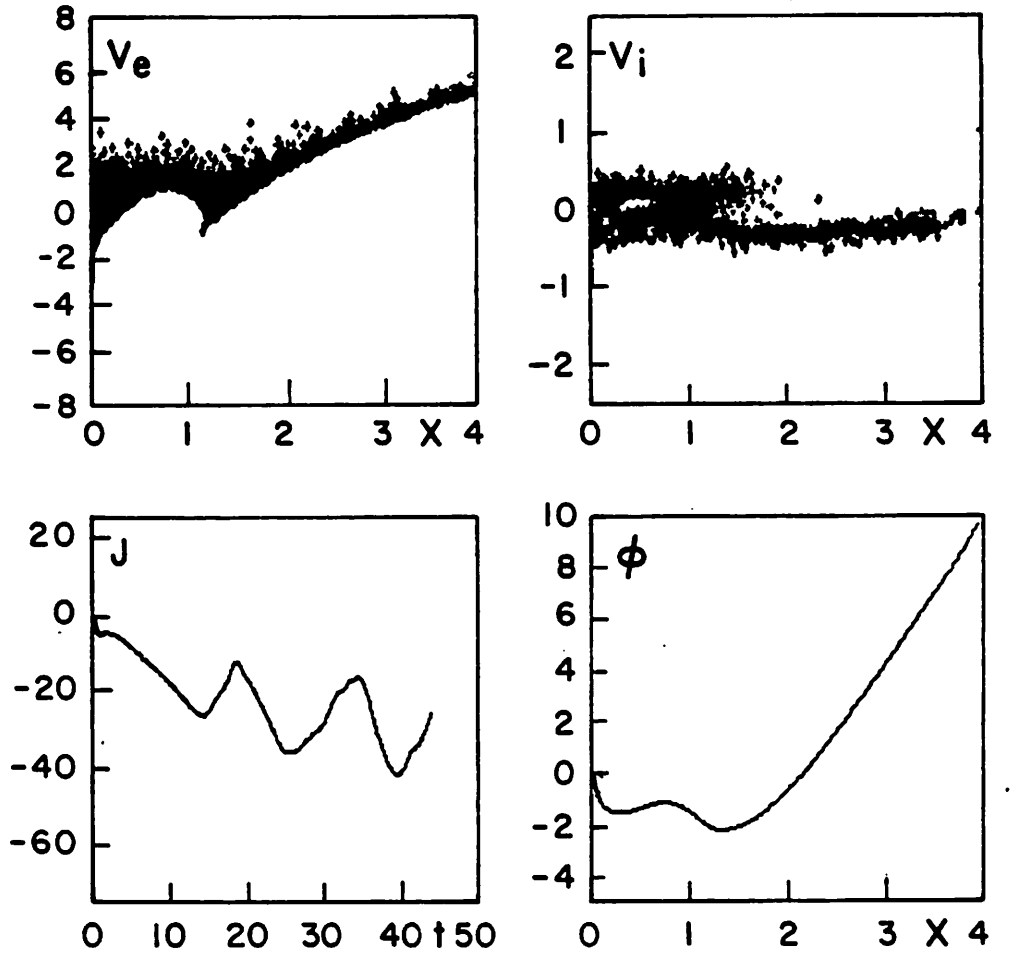

Fig 4. Run 3, electron rich, at t = 43.75. The lower left is now J(t) showing a relaxation-like oscillation. The second potential minimum in φ has just caused some electrons to begin to form an electron hole, as seen in v_e-x space. The oscillation period is a little shorter than a thermal ion transit time.

This is the same model as in Runs R2 and R3, except half as long, making it stable.

Run R5. Ion rich, $\alpha = 4.0$, floating collector.

The ion-richness causes formation of a potential maximum (virtual anode) in front of the source (ion Debye cloud) which then drops off toward the collector, which is again charged negatively. In analogy with R4, it is expected that an electron hole would form, but it does not, filling in nicely, amost with a full Maxwellian distribution, as appearing in the lower left hand corner plot. This filling is puzzling, coming, say, from time-varying fluctuations (time-independent energy conservation does not allow filling) or nonlinear dynamics, or simply due to the initiation from vacuum conditions with very large potential changes. Because φ_{max} and φ_{plasma} remain the same as the number of particles increased considerably, the timestep is reduced, the mesh is made finer, it is believed that the hole-filling is not a numerical artifact.

Figure 5 shows a movie-like set of snapshots of e and i phase spaces, charge density ρ, and potential φ, at t = 50. An electron hole is expected from the virtual anode region (located $0 < x \lesssim 0.4$), with the slowest electron injected (v = 0) accelerated to energy $e\varphi_{max}$.

The mean number of ions is about 5600 and the mean number of electrons is about 5300, still rising slowly at the end of the run. In subsequent much longer runs, the electron hole region is found to expand across the device, with the positive potential region also continuing across the device; there is a core of cooler electrons almost all across the device, surrounded by much warmer electrons.

Runs R6, R7. Ion-rich, $\alpha = 4$, small positive bias, net current.

The potential maximum here allows all electrons to flow into the device, with the ions penetrating quite far. Then too many electrons are drawn in, a

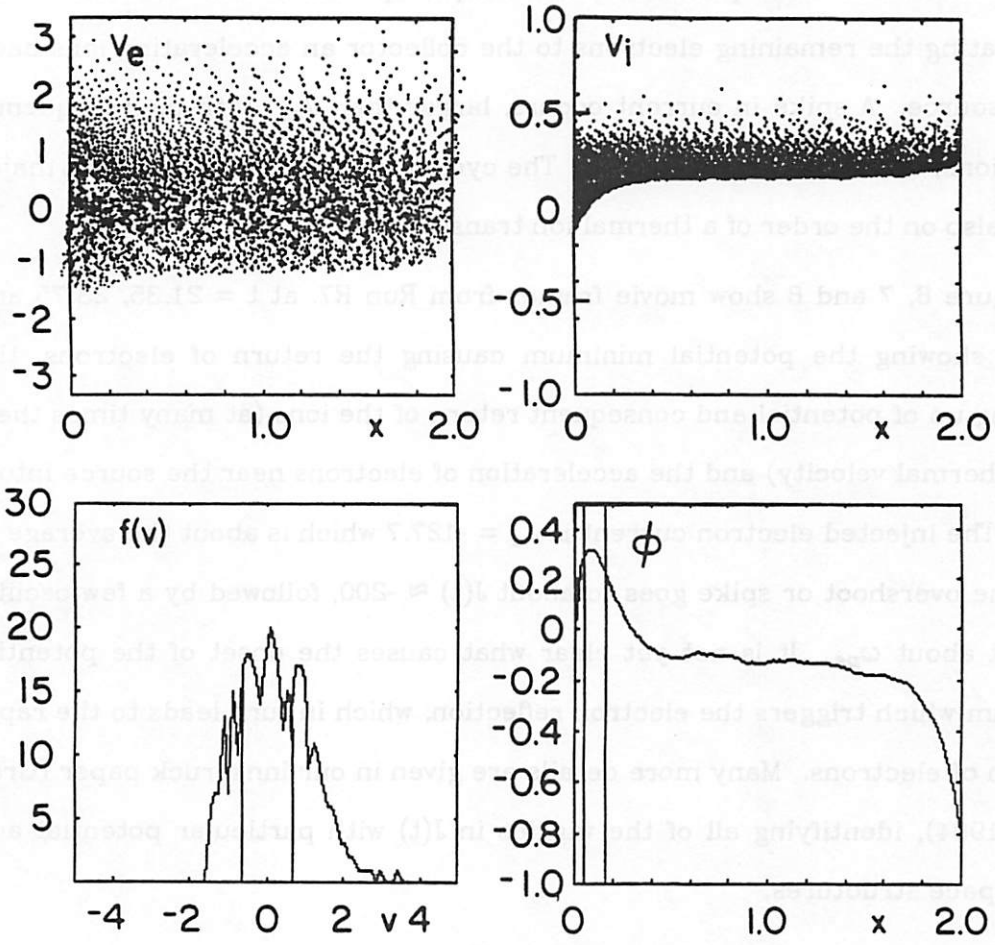

Fig 5. Run R5, ion rich, at time t = 20. The lower left is the electron distribution function measure between x = 0.04 and x = 0.16, where an electron hole was expected (due to the virtual anode seen in φ). Instead, there is the near Maxwellian shown here.

very small potential minimum forms, instantly returning and ejecting some excess electrons. The potential then snaps up above the vacuum value, accelerating the remaining electrons to the collector an accelerating ions back to the source. A spike in current occurs, larger than J_{e0}, with high frequency oscillations; then the current decays. The cycle repeats as in R2, R3, with major period also on the order of a thermal ion transit time.

Figure 6, 7 and 8 show movie frames from Run R7. at t = 21.35, 23.75 and 28.125, showing the potential minimum causing the return of electrons, the snapping up of potential and consequent return of the ions (at many times their initial thermal velocity) and the acceleration of electrons near the source into a beam. The injected electron current is J_e = -127.7 which is about the average of J(t). The overshoot or spike goes to about J(t) ≈ -200, followed by a few oscillations at about ω_{pe}. It is not yet clear what causes the onset of the potential minimum which triggers the electron reflection, which in turn leads to the rapid ejection of electrons. Many more details are given in our Innsbruck paper (Gray et al., 1984), identifying all of the wiggles in J(t) with particular potential and phase space structures.

Run R8. Ion rich, α = 4.0, large positive bias.

There is still a positive maximum, letting all electrons in, but so large a positive bias that ions hardly penetrate the device. The result is a stable almost Child's law potential electron diode, with φ (x) $\sim x^{4/3}$. There is no plasma plateau.

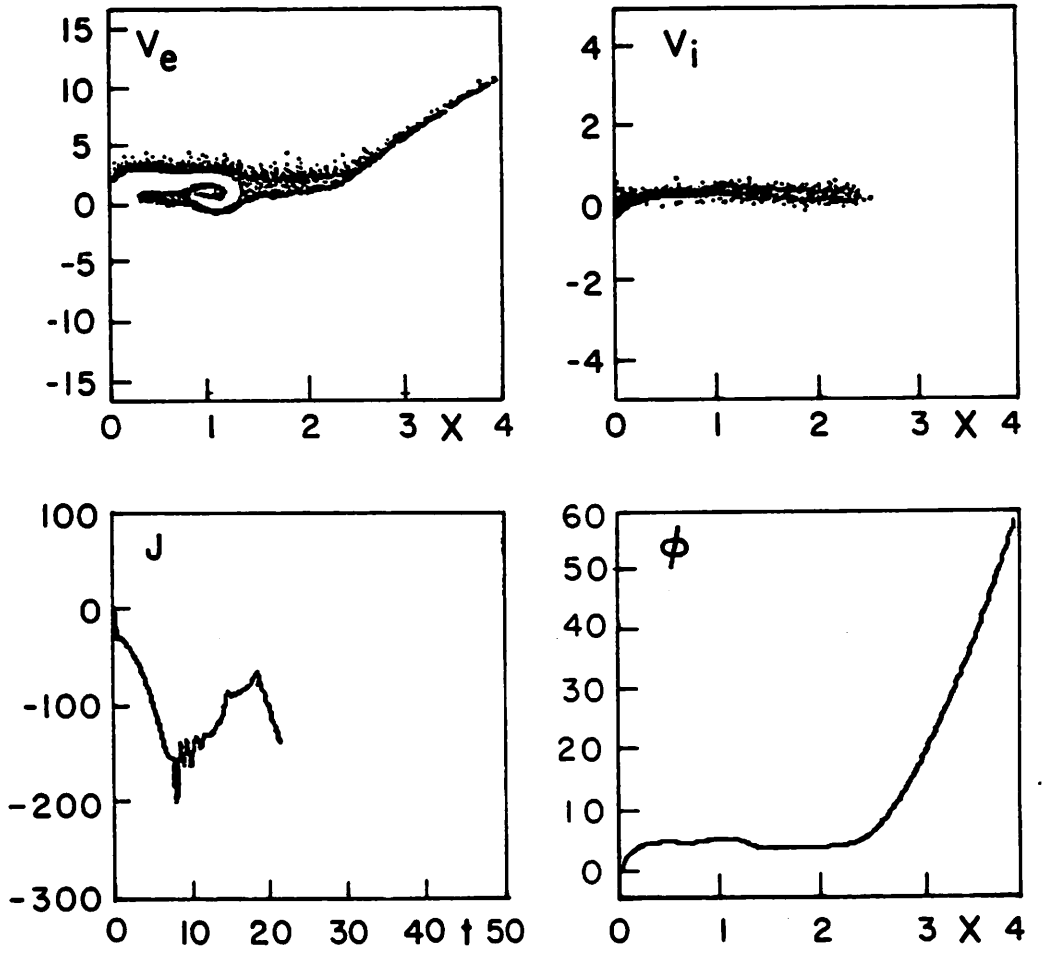

Fig 6. Run R7, ion rich, at time t = 21.25. The small potential minimum in φ has caused some electrons to form the vortex seen in v_e-x space. The current, lower left, shows peak larger than the injected electron current, followed by fast oscillations (near ω_{pe}) and relaxation.

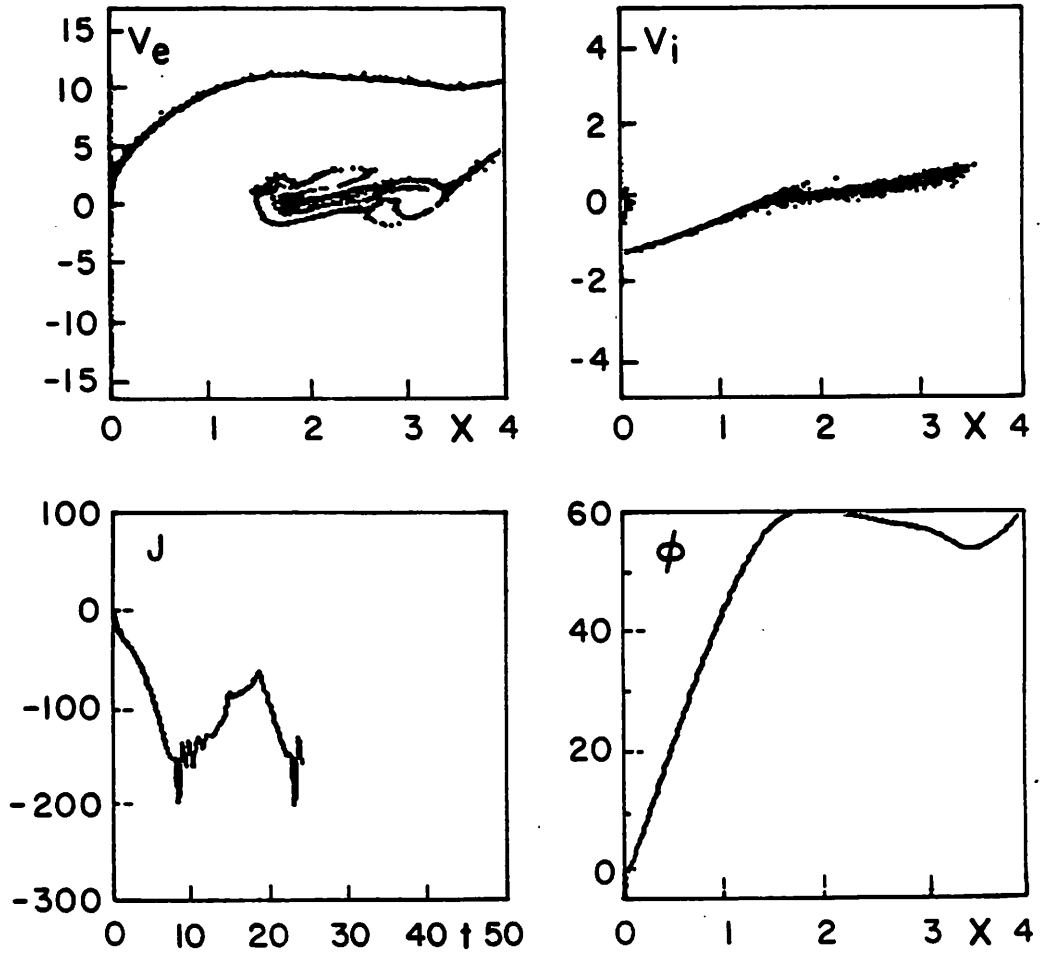

Fig 7. Run R7 at time t = 23.75, showing development of the oscillation observed in Figure 6. The electron vortex is leaving on the right. The ions are accelerated back toward the source, reaching about ten times their injection speed. The potential rises above that applied. The main oscillation period is a little shorter than a thermal ion transit time.

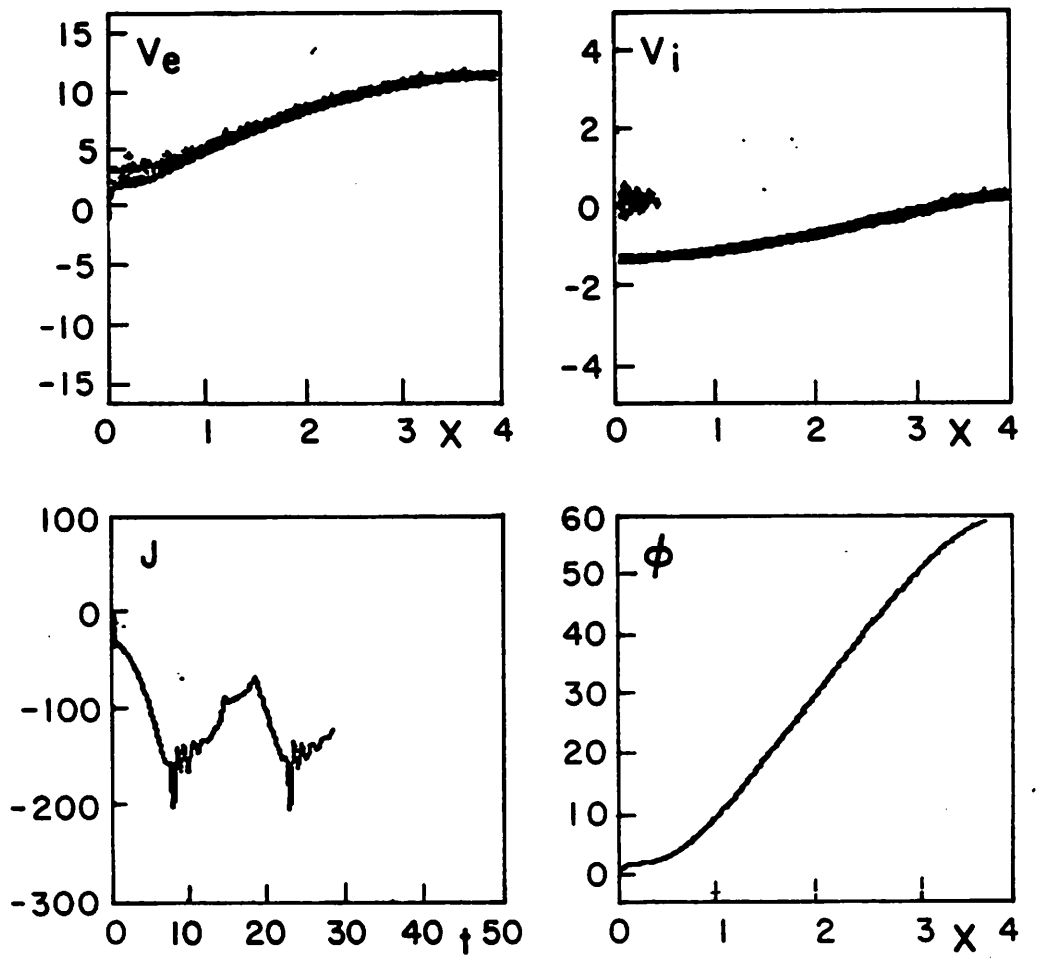

Fig 8. Run R7 at time t = 28.125. The electron vortex has been collected; the ions are still draining out to the source. The sequence repeats again and again.

Appendix A

PDW1 Computer Simulation Code

PDW1 is a one dimensional, magnetized, electrostatic particle simulation with one, two or three velocity coordinates, and non-periodic boundary conditions. It is set up to inject particles with Maxwellian distributions with arbitrary drift velocities and cut-off velocities, but is easily modifiable to suit other distributions.

PDW1 is an acronym for Plasma Device Workshop. The code was written during, and for use in, a seminar workshop at the University of California at Berkeley on axially bounded plasma systems during the 1983 spring quarter.

The purpose of PDW1 is to solve electrostatic magnetized plasmas with non-periodic boundary conditions. Inherent in non-periodic boundary conditions is an external circuit of some sort, and working this external circuit into the code was the major step forward. Figure A1 is a diagram of the model. Specifically, the equations to be solved are:

$$\frac{d^2x_i}{dt^2} = \frac{q_i}{m_i} E(x_i,t)$$

where x_i, q_i and m_i are the position, and charge and mass sheet densities of the i'th particle respectively. E is the x directed electric field, obtained from

$$\frac{\partial E}{\partial x} = \frac{1}{\varepsilon_0} \sum_i q_i S_i(x - x_i)$$

where S_i is the shape factor for the i'th particle (ε_0 is the dielectric constant in a vacuum).

$$\hat{L}\,\frac{dI}{dt} + \hat{R}I + \frac{Q}{C} + V_0(t) = V(t)$$

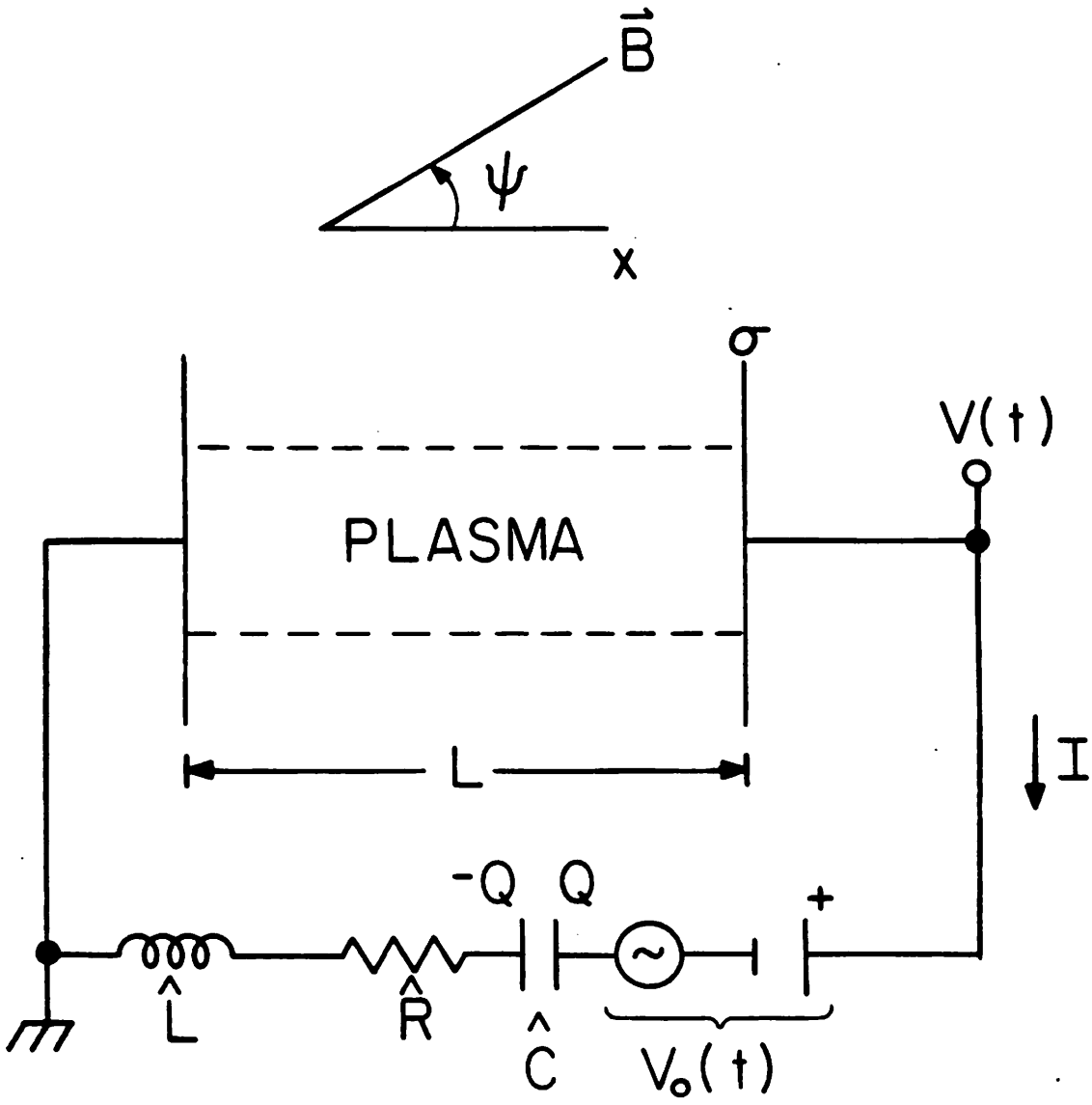

Fig A1. Diagram of the PDW1 model.

where $\hat{L}$, $\hat{R}$, and $\hat{C}$ are the inductance, resistance, and capacitance of the external circuit, V_0 is a source voltage, V is the voltage across the plasma region, and I and Q are the current and charge associated with the external circuit (Q is the charge on the capacitor) such that I = dQ/dt. Finally

$$\frac{d\sigma}{dt} = \sum_i q_i v_i \delta(x_i - L_x) - \frac{I}{A}$$

where σ is the charge on the plate at the right hand boundary of the plasma region, A is the area of that plate, v_i is the velocity of the i'th particle, and L_x is the length of the plasma region. The factor of area of the end plate is necessary because σ is a surface charge density. This last equation determines the boundary condition for the field solve, since

$$E(L) = -\frac{\sigma}{\varepsilon_0} .$$

All these equations have initial conditions, which can be specified.

In addition to all these equations, the injection and initial loading of particles must be specified (see Figure A2). PDW1 is currently set up to load and inject partial Maxwellian distributions, but the loading scheme is capable of handling almost any distribution. The Maxwellian distributions injected at each end (independently) can be offset (representing a drift velocity) and cut off at any velocity greater than zero (or less than zero for the right hand wall) to represent a distribution which has already been accelerated (see Figure A3).

PDW1 is descended from the periodic code ES1 which is thoroughly described in Chapters 1-5 *Plasma Physics Via Computer Simulation* by Birdsall and Langdon (McGraw-Hill, 1985). The bounded features of PDW1 are touched on in Chapter 16.

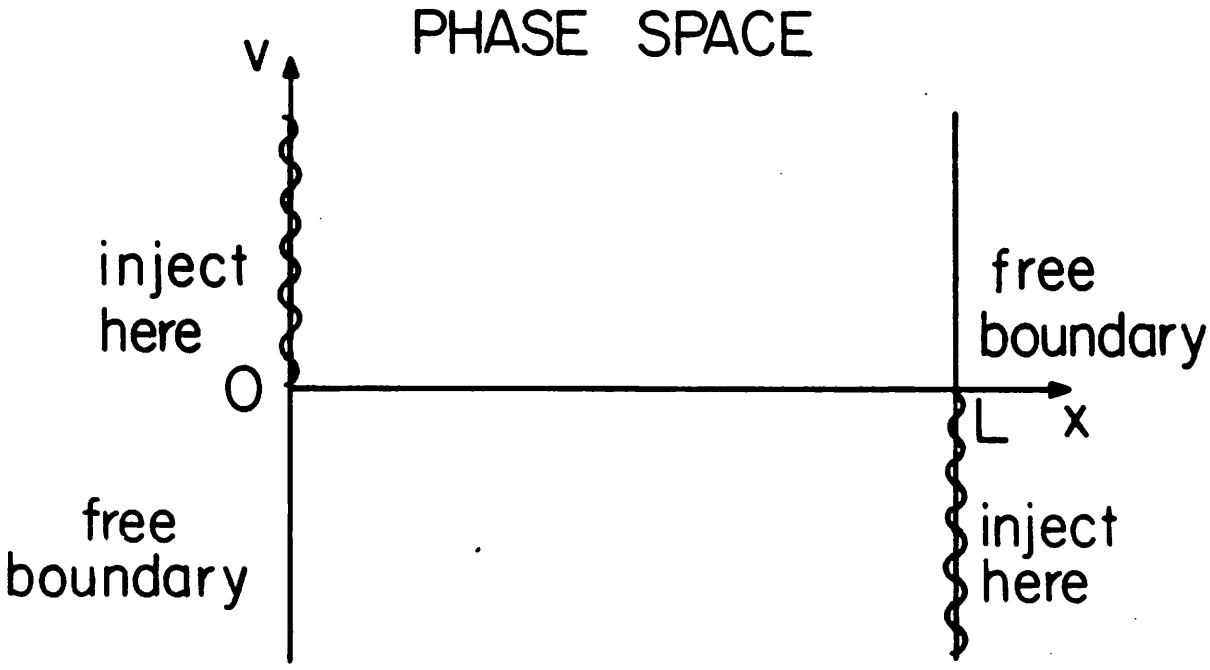

Fig A2. Phase space boundaries.

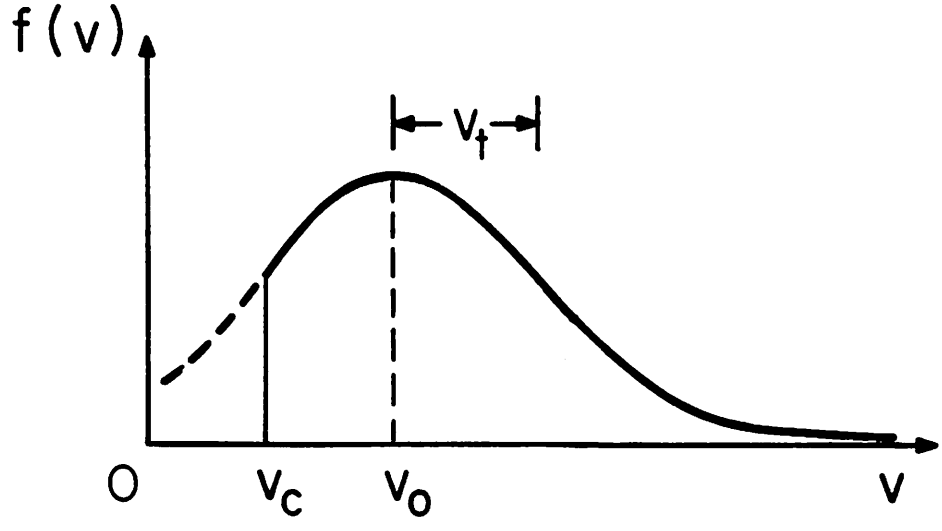

Fig A3. Injected distribution.

Readers interested in using PDW1 should obtain PDW1 USER'S MANUAL by W. S. Lawson, ERL Memorandum UCB/ERL M84/37, 27 April 1984, by writing to Professor C. K. Birdsall.

Appendix B

Table II: Computer Parameters

For all runs:

NSP = 2, NV = 1, AREA = 1.0, ESPO = 1.0, IOUT = 200, IHIST = 400, IPACK = 10, ZED = 0, Zero for variables B, PSI, RHOBACK, BACKJ, EXTR, EXTL, ACBIAS, WO, QO, IO, SIGMAO. Zero for electron and ion species variables VOL, VOR, VCR, VYL, VYR, VZL, VZR

For electrons

$$FLUXL = n_{eo}^{+} \bar{v} = n_{eo}^{+} \sqrt{\frac{2}{\pi}}\ v_{te}$$

$$JOL = q_e n_{eo}^{+} \bar{v} = q_e n_{eo}^{+} \sqrt{\frac{2}{\pi}}\ v_{te}$$

For both species, all runs set EMPTY and INJECT equal to .TRUE.

Run No.	R1	R2/R3	R4	R5	R6/R7	R8
EXTC	0	1E+20	1E+20	0	1E+20	1E+10
DCBIAS	0	10.0	10.0	0	60.0	150.0
ISAV	16	40	16	16	80	40
LXMAX	96	10	25	10	10	10
LXMIN	32	3	6	3	3	3
<u>ELectron species</u>						
JOL	63.8305	127.661	127.661	63.8305	127.661	127.66
FLUXL	1276.61	2553.22	2553.22	1276.61	1276.61	1276.61
<u>Ion Species</u>						
JOL	10.092	2.0184564	2.0184565	40.36985	80.73626	80.73626
FLUXL	201.844	40.3691	40.3691	807.399	807.3626	807.3626

Section VI. References

The references listed here are only a few of those pertaining to the subject of the text. However, they provide a fair sampling of early works, including theory, simulation and experiment.

Reports are in preparation by members of the Berkeley Plasma Theory and Simulation Group providing more details of several of the sequences shown in the movie, expanding on the brief descriptions given here and our various conference papers, and offering some theory.

Birdsall, C. K., "Plasma-Sheath-Wall Time-Dependent Behavior - An Informal Survey," ERL Memo No. UCB/ERL M82/51, 22 June 1982 (University of California, Berkeley).

Birdsall, C. K., and W. B. Bridges, *Electron Dynamics of Diode Regions*, Academic Press N. Y. (See especially Chapter 3 on virtual cathode formation and oscillation and prior references.) 1966.

Birdsall, C. K., T. L. Crystal, P. C. Gray, and S. Kuhn, "Instability of a Collisionless Single-Ended Plasma Device Operated in the Positive-Bias Electron-Rich Regime, from Simulations," 17th International Conference on Phenomena in Ionized Gases, Budapest, Hungary, July 1985.

Burger, P., "Nonexistence of dc States in Low-Pressure Thermionic Converters," Jour. Appl. Phys. **35**, pp. 3048-3049, 1964.

Burger, P., "Theory of Large-Amplitude Oscillations in the One-Dimensional Low-Pressure Cesium Thermionic Converter," Jour. Appl. Phys. **36**, pp. 1938-1943, June 1965.

Burger, P., "Zero-Field Solutions and Their Stability in the One-Dimensional Low-

Pressure Cesium Diode," Jour. Appl. Phys., **38**, pp. 3360-3368, July 1967.

R. Chodura, "Plasma-Wall Transition in an Oblique Magnetic Field, Phys. Fl. **25**, pp. 1628-1633, September 1982.

R. Chodura, "Plasma-Flow in the Sheath and the Presheath of a Scrape-off Layer," IPP 5/1 Feb 1985, Max Planck Inst. für Plasmaphysik, Garching bei München, F.R.G.

R. Chodura, "Electron Energy Flow in a Collisional Scrape-off Plasma," 12th European Conf. on Plasma Physics, Budapest, Hungary, Sept. 1985.

Cutler, W. H., "High Frequency Oscillations in a Thermal Plasma," Jour. Appl. Phys. **35**, pp. 464-465, 1964.

Cutler, W. H., and P. Burger, "Oscillations in the Thermal Cesium Plasma Diode," Jour. Appl. Phys. **37**, pp. 2867-2873, June 1966.

Gray, P. C., S. Kuhn, T. L. Crystal, and C. K. Birdsall, "Particle Simulations of the Unstable States of a Collisionless Single-Ended Plasma Device," Paper O-6, Second Symposium on Plasma Double Layers and Related Topics, (p. 266 of Proceedings) Innsbruck, Austria July 5-6, 1984.

Iizuka, S., P. Michelsen, J. J. Rasmussen, R. Schrittwieser, R. Hatakeyama, K. Saeki, and N. Sato, "Dynamics of a Potential Barrier Formed on the Tail of a Moving Double Layer in a Collisionless Plasma," Phys. Rev. Lett. **48** pp. 145-148, 18 January 1982. (Also see comments on this letter by Kuhn, PRL p. 217, reply by authors p. 218, 17 January 1983.)

Iizuka, S., and H. Tanaca, "Nonlinear Evolution of Double Layers and Electron Vortices in an Unstable Plasma Diode," J. Plasma Physics, **33**, pp. 29-41, 1985.

Kuhn, S., "Axial Equilibria, Disruptive Effects, and Buneman Instability in Collisionless Single-Ended Q-Machines," Plasma Physics 23 pp. 881-902, 1981.

Kuhn, S., C. K. Birdsall, T. L. Crystal, P. C. Gray, and Wm. S. Lawson, "One-Dimensional Particle Simulations of the Collisionless Single-Ended Q Machine," Paper P8-11, 1984 International Conference on Plasma Physics, (p. 104 of Proceedings Contributed Papers), Lausanne, Switzerland, June 27-July 3, 1984b.

Kuhn, S., P. C. Gray, T. L. Crystal and C. K. Birdsall, "Axial Equilibria of Collisionless Single-Ended Q-Machines: Particle Simulation versus Theory and Experiment," Paper 5Q6, 1984 IEEE International Conference on Plasma Science (p. 119 of Conference Record) St. Louis, Missouri May 14-16, 1984a.

Kuznetsov, V. I., and A. Ya. Ender, "Nonlinear Oscillations in a One-Dimensional Bounded Knudsen Plasma," Sov. Phys. Tech. Phys. **22**, 1295-1300, 1977.

Kuznetsov, V. I., and A. Ya. Ender, "Calculation of Nonlinear Self-Consistent Oscillations and the Ion Distribution Function," Sov. Phys. Tech. Phys. **28**, 1431, 1983.

Ott, W., "Investigation of a Caesium Plasma Diode Using an Electron Beam Probing Technique," Z. für Naturforschung **22**, pp. 1057-1067, 1967.

Rynn, N., "Current-Induced Effect in an Alkali-Metal Plasma," Jour. Appl. Phys. **5** pp. 634-636, May 1982.

Rynn, N., "Plasma Column End Effects," Phys. Fl. **9** pp. 165-176, January 1966.